Nanoscale Res Lett (2010) 5:753–760
DOI 10.1007/s11671-010-9553-x

NANO EXPRESS

CdTe Quantum Dot/Dye Hybrid System as Photosensitizer for Photodynamic Therapy

Aliaksandra Rakovich · Diana Savateeva · Tatsiana Rakovich · John F. Donegan · Yury P. Rakovich · Vincent Kelly · Vladimir Lesnyak · Alexander Eychmüller

Received: 16 December 2009 / Accepted: 28 January 2010 / Published online: 10 February 2010
© The Author(s) 2010. This article is published with open access at Springerlink.com

Abstract We have studied the photodynamic properties of novel CdTe quantum dots—methylene blue hybrid photosensitizer. Absorption spectroscopy, photoluminescence spectroscopy, and fluorescence lifetime imaging of this system reveal efficient charge transfer between nanocrystals and the methylene blue dye. Near-infrared photoluminescence measurements provide evidence for an increased efficiency of singlet oxygen production by the methylene blue dye. In vitro studies on the growth of HepG2 and HeLa cancerous cells were also performed, they point toward an improvement in the cell kill efficiency for the methylene blue-semiconductor nanocrystals hybrid system.

Keywords Quantum dots · Nanocrystals · Photosensitiser · Electron transfer · Singlet oxygen

A. Rakovich · J. F. Donegan · Y. P. Rakovich (✉)
School of Physics and CRANN Research Centre, Trinity College, Dublin 2, Ireland
e-mail: Yury.Rakovich@tcd.ie

D. Savateeva
Brest State Technical University, 224017 Brest, Belarus

T. Rakovich · V. Kelly
School of Biochemistry and Immunology, Trinity College, Dublin 2, Ireland

V. Lesnyak · A. Eychmüller
Physikalische Chemie/Elektrochemie, TU Dresden, Bergstr. 66b, 01062 Dresden, Germany

Introduction

Methylene blue (MB) is a dye that has been extensively used for a variety of photochemical [1] and medical applications [2], including photodynamic therapy (PDT). In PDT, it acts as a photosensitizer for the production of singlet oxygen [1] (O_2) through energy transfer between its excited triplet state and the ground triplet state of molecular oxygen. It has been suggested that singlet oxygen may be linked to apoptosis of cancerous cells, while oxygen free-radicals are more likely to cause necrosis [2]. Apoptosis is a more favorable cell death mechanism, since it includes a safe disposal of cellular debris. Necrosis, on the other hand, is a form of traumatic cell death and often leads to inflammation and other complications. The use of MB in PDT has been limited by the formation of MB dimers [3] and the reduction in MB to the photochemically inactive leuco-MB under physiological conditions [4], both of which result in a decreased efficiency of singlet oxygen production. In this work, we attempt to increase this efficiency by addition of CdTe nanocrystals (NCs).

Semiconductor nanocrystals (NCs), otherwise known as quantum dots (QDs), are promising for such applications because of their size-dependent optical properties [5]. They have wide absorption bands and relatively narrow, tunable emissions, which makes them ideal candidates as Förster resonance energy transfer (FRET) pairs. The shell of ligand molecules surrounding the NCs allows their chemical properties to be adjusted through relatively straightforward solution-based surface chemistry [6]. On the basis of their versatility and unique optical properties, semiconductor nanocrystals are impacting the areas of photonics [7, 8], electronics [8], and bio-imaging [8, 9].

Experimental Methods

Materials and Sample Preparation

Methylene blue dye powder was bought from Sigma–Aldrich. Thioglycolic acid (TGA)-stabilized CdTe NC samples were prepared by an aqueous method as reported previously [10, 11]. Both the dye and the NC samples were diluted in water to give 1×10^{-5} M stock solutions. Doubly purified deionized water from an 18 MΩ Millipore system was used for all dilutions.

Two CdTe samples were used, with emissions centered at 545 nm and 645 nm (Fig. 1a). These emission maxima correspond to NC sizes of 2.8 nm and 3.3 nm, respectively, as calculated according to Peng [12]. Both of these samples were diluted to give 10^{-5} M stock solutions and then mixed with a 10^{-5} M MB stock solution to give two sets of mixtures of increasing MB concentrations. To aid the reference to the samples, each set was labeled with NC size (2.8 or 3.3 nm) and then letters "a"–"g" corresponding to ∞, 10:1, 5:1, 1:1, 1:5, 1:10, 0 QD:MB molar ratios, respectively. QD solutions were sonicated for approximately 5 min prior to mixing.

For work with cancerous cells, the 3.3-nm NC sample was diluted to give a 5×10^{-6} *M* solution and five MB solutions of different concentrations were also prepared (Table 1). HepG2 and HeLa cells, obtained from the European Collection of Cell Cultures, were grown in serum-free medium ultra culture (Lonza) at 37°C in a 5% CO_2 humidified atmosphere. Cells were seeded onto 96 wells of a 96-well plate (5,000–10,000 cells per well). To each of the well, 5 μL of QD solution and/or 5 μL of MB solution were added, as summarized in Table 1. The plate was placed approximately 10 cm away from a standard UV lamp for varying periods of time (30–180 s). The cells were then washed with fresh ultra culture solution, and incubated for 24–32 h. After the incubation, cells were counted using fluorescent labeling with a CyQuant Cell Proliferation Assay Kit (Biosciences).

Measurements

Absorption spectra were recorded on a Varian Cary50Conc UV–visible spectrophotometer. Steady-state photoluminescence measurements were taken using a Varian Cary-Eclipse Fluorescence Spectrophotometer ($\lambda_{ex} = 400$ nm). Near-infrared (NIR) photoluminescence spectra were recorded on FLS920 fluorescence spectrometer (Edinburgh Instruments) with a Hamamatsu R5509 NIR photomultiplier tube. For these measurements, both the nanocrystals and methylene blue powders were dissolved in deuterium oxide (D_2O): this increases the lifetime of singlet oxygen in solution and allows it be detected spectroscopically.

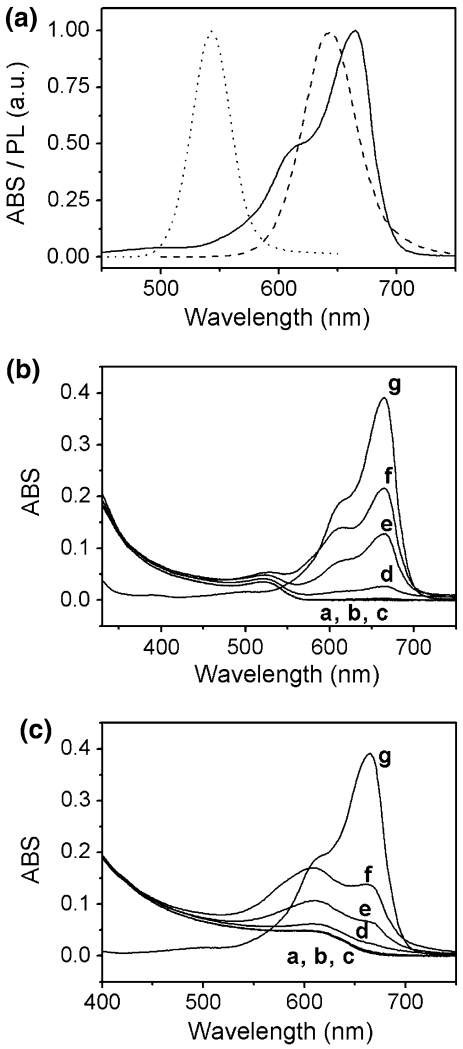

Fig. 1 Spectroscopic measurements of methylene blue-CdTe nanocrystals solutions. Panel **a** normalized absorption spectrum of methylene blue dye (*solid line*) and photoluminescence spectra of 2.8-nm (*dotted line*) and 3.3-nm (*dashed line*) colloidal CdTe samples. The 2.8-nm NCs have much smaller spectral overlap with methylene blue. Panels **b** and **c** show the change in the absorption spectrum of **b** 2.8-nm and **c** 3.3-nm CdTe NCs with increasing dye concentration (curves "a"–"g"), respectively. There was no evidence of any major chemical changes upon the mixing of NCs and MB dye

A Malvern NanoZS was used for zeta potential measurements. PL decays were measured using time-correlated single photon counting utilizing a PicoQuant MicroTime200 set-up. Measurements were taken in ambient conditions, at room temperature, on solutions diluted to yield reasonable signal intensity. Samples were excited by a 480-nm picosecond laser pulse (PicoQuant LDH-480 laser head controlled by PDL-800B driver). The overall resolution of the setup was ~150 ps. The measured PL decays were reconvoluted using non-linear least-squares analysis. This was done with SymPhoTime software (PicoQuant) using an equation of the form

Table 1 Experimental setup used to study the effect of NC–MB mixtures on the growth of cancerous cells

Line no.	Sample description
1	Control (no QD/MB)
2	QD only control
3	MB only (1:1)
4	MB only (5:1)
5	MB only (10:1)
6	MB only (20:1)
7	MB only (30:1)
8	MB and QD (1:1)
9	MB and QD (5:1)
10	MB and QD (10:1)
11	MB and QD (20:1)
12	MB and QD (30:1)
MB:QD ratio	**MB concentration (M)**
1:1	5×10^{-6}
5:1	2.5×10^{-5}
10:1	5×10^{-5}
20:1	1×10^{-4}
30:1	1.5×10^{-4}

A 96-well plate was divided into 12 rows each containing 8 repeats of different samples, as summarized in the table. MB:NC molar ratios and corresponding concentrations of MB solutions that were used in these experiments are also given

$$I(t) \propto \sum_i \alpha_i \exp(-t/\tau_i) \tag{1}$$

Where τ_i are the PL decay lifetimes and α_i are the corresponding pre-exponential factors, taking into account the normalization of the initial point in the decay to unity. Weighted residuals and χ^2 values were used to judge the quality of the fit. A fit with χ^2 value of less than 1.1 was considered to be good. The τ_i and α_i values obtained from the fit were then used to calculate the average lifetime τ_{av} using the following equation:

$$\tau_{\text{av}} = \frac{\sum \alpha_i \tau_i^2}{\sum \alpha_i \tau_i} \tag{2}$$

Fluorescence correlation spectroscopy (FCS) measurements were taken on a MicroTime 200 confocal microscope (PicoQuant) fitted with an oil immersion objective. Appropriately diluted samples were excited with a 480-nm pulsed laser diode (LDH-480) with a repetition rate of 80 MHz. Measurements were taken at room temperature with total acquisition times of about 1 min. The data was stored in the time-tagged time-resolved mode (TTTR) and then analyzed using SymPhoTime software (PicoQuant). A pure diffusion fitting model was employed. In this case, only the diffusion of fluorophores contributes toward the correlation curve, and the FCS intensity ($G(t)$) is given by

$$G(t) = \sum_{i=1}^{n} \rho_i \left(1 + \frac{t}{\tau_i}\right)^{-1} \left(1 + \frac{t}{\tau_i \kappa^2}\right)^{-1/2} \tag{3}$$

Where t is the lag time, τ_i the diffusion time of the ith diffusing species, and ρ_i the contribution of ith species. κ is the length to diameter ratio of the focal volume ($V_{\text{eff}} = \pi^{3/2} w_0^2 z_0$), where w_0 and z_0 are the effective lateral focal radius and focal radius along the optical axis at e^{-2} intensity, respectively. Once τ_i and w_0 were determined, the diffusion constant, D_i, of the ith species was calculated using

$$D_i = \frac{w_0^2}{4\tau_i} \tag{4}$$

Results and Discussion

Absorption Spectra

Figure 1b and c show absorption spectra for 2.8 nm and 3.3 nm sets, respectively. The absorption spectra of 2.8-nm NC/MB samples appear to be linear combinations of the NC and dye absorptions, suggesting that no major chemical changes occur upon mixing. At 664 nm, the absorption for samples "f" for both NC sizes was less than those of samples "g", despite the fact that the concentration of the dye in these samples was the same. This is equivalent to saying that the amount of methylene blue monomers (absorb at 664 nm) in NC solutions is less than if NCs were not present. This suggests that some dimerization of dye molecules occurs, with a subsequent increase in absorption at 613 nm (dimer absorption). This result is consistent with previous findings that the presence of interfaces (surfaces) causes the partial dimerization of methylene blue [3]; it also suggests that MB molecules *adsorb* onto the nanocrystal surface. This is not surprising since there is an electrostatic attraction between the positively charged MB and negatively charged TGA-capped CdTe NCs.

Steady-state and Time-resolved Photoluminescence Measurements

Steady-state PL measurements showed a decrease in luminescence intensity for both CdTe samples as the concentration of MB was increased (Fig. 2a and b). Complete quenching was observed at NC to MB ratio of about 1–10 in both cases (samples f). The 3.3-nm CdTe NCs were quenched faster (Fig. 2b), i.e., less MB molecules were required to quench the luminescence of this sample by the same amount. Assuming that in this system, quenching occurs through Föster resonance energy transfer (FRET),

this difference could be attributed to the lesser overlap of 2.8-nm NC emission band and MB absorption band compared to 3.3-nm NCs (Fig. 1). However, typically, FRET results in an enhanced emission from the fluorescent acceptor [13] (in this case, the MB dye). This was not observed for either of the samples. In fact, at 480-nm excitation, the MB luminescence was also found to be fully quenched (inset of Fig. 2a).

Lifetime measurements are often taken in order to confirm the occurrence of energy transfer – a decrease in the average lifetime of donor is expected for nanocrystal luminescence quenching [14]. As seen in Fig. 3, no change in the lifetime of 2.8-nm NCs was detected and a very small decrease in the lifetime of the 3.3-nm NCs was observed. Taking into account the large difference in the spectral overlap between MB absorption and QD emission spectra for the two samples, we expected a much larger difference in the behavior of PL decays for the two series. Thus, PL decay measurements confirm that FRET cannot be fully responsible for the observed effect but may contribute to the quenching of luminescence for the 3.3-nm QD sample.

Quenching Mechanism

Upon the inspection of band off-sets for MB and NCs [15] (Fig. 4), we have concluded that, for this system, photo-induced charge transfer (PCT) is the most likely mechanism of luminescence quenching. The evidence for the *photoinduction* can be derived through the comparison of the PL spectra of the 2.8-nm NC series when excited at 480 nm and 633 nm (Fig. 2a and c, respectively). As discussed previously, when NC/MB mixtures were excited at 480 nm, complete quenching of the dye luminescence was observed. At 633 nm, the CdTe NCs are not excited and a PL signal due to the dye (680-nm region) was detected. The signal increased in proportion to the absorption value of the samples at the excitation wavelength (Fig. 1b). The inset of Fig. 2c shows PL spectra normalized based on absorption at 633 nm for samples "f" and "g" of the series (these samples have equal MB concentrations). The PL intensity was found to be same for both samples, indicating a lack of quenching at this excitation wavelength.

Adsorption of Methylene Blue on NC Surface

A close proximity of two interacting moieties is a necessity for charge transfer to occur between them [16]. This implies that QDs and MB do indeed associate, concurring with proposal reached upon the inspection of the absorption data (earlier). Non-linear Stern–Volmer plots, derived from the PL data at 480-nm excitation (Fig. 5a and b), are in support of this since such concave upward curves

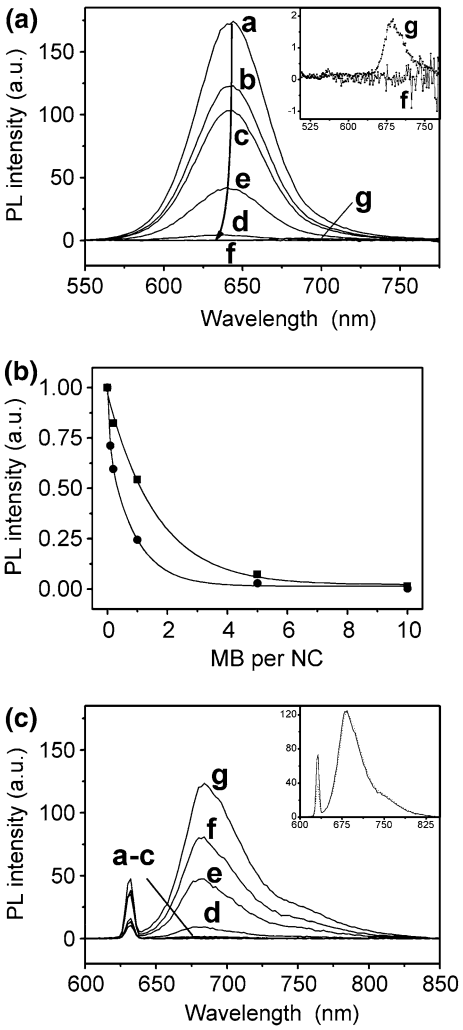

Fig. 2 Changes in the photoluminescence of CdTe nanocrystals upon the addition of methylene blue. Panel **a** Quenching of PL of 3.3-nm CdTe NCs solution at increasing dye concentration ("a"–"g"). Inset: PL spectra for samples "3.3 f" and "3.3 g" reveal the complete quenching of dye molecules. Panel **b** Comparison of photoluminescence quenching curves for 2.8-nm and 3.3-nm NCs samples. Photoluminescence intensity against the number of MB molecules per NC for 2.8-nm (*closed square*) and 3.3-nm (*closed circle*) NCs shows that 3.3-nm NCs are quenched more by the same number of MB molecules. Difference could be attributed to the larger spectral overlap with dye's absorption band for this NCs sample. Panel **c** Photoluminescence measurements of 2.8-nm CdTe NCs/MB mixtures at 633-nm excitation. At 633-nm excitation, the NCs are not excited and only emission from MB is observed, which decreases in accordance with the concentration of MB in samples "a"–"g". The inset shows the emission spectra of the last two samples in the 2.8-nm NC series, normalized on absorption at excitation wavelength (633 nm). The two spectra overlap each other, so there is no quenching of MB emission when QDs are not excited

indicate that both static and dynamic quenching take place [17]. Further more, the fact that lifetime SV data is much smaller than the corresponding intensity SV data suggests that static quenching dominates in this system. The Stern–Volmer plot for 2.8-nm NC/MB set was found to be less

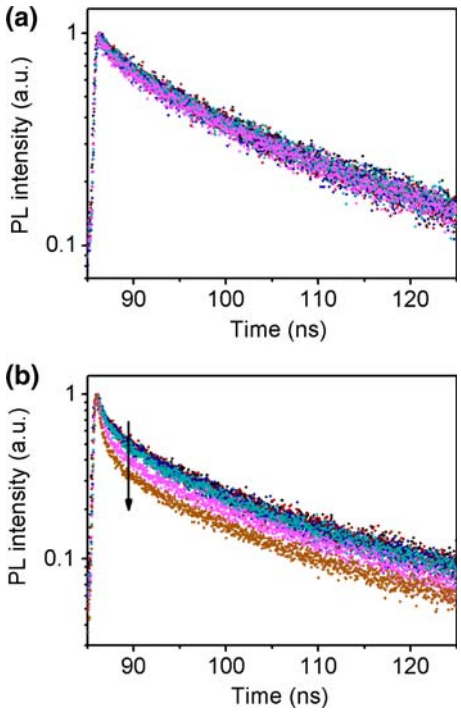

Fig. 3 Time-resolved PL decay measurements on NC–MB mixtures. Panels **a** and **b** show PL decay data for 2.8-nm and 3.3-nm NC–MB mixtures at increasing NC–MB molar ratios, respectively. No change in the photoluminescence decay behavior was detected for 2.8-nm NCs, and only a small decrease in the shorter component of the decay was observed for 3.3-nm NCs (indicated by an *arrow*). This suggest that energy transfer only occurs for 3.3-nm NCs, for which spectral overlap was significant

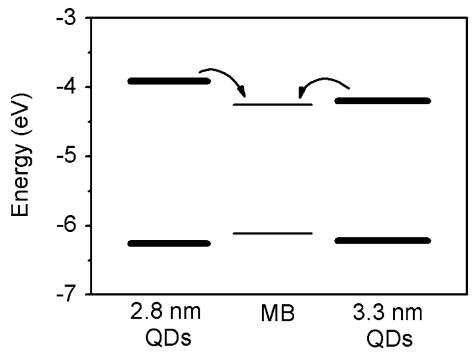

Fig. 4 Energy band off-sets for MB and the two NCs samples allow for charge transfer between the NCs and the dye

concave. In all likelihood, the differences in quenching behavior of the two NC samples arise because of the FRET contribution to the quenching of 3.3-nm NC sample.

Several additional measurements were taken to validate MB adsorption onto QDs. First, the dependence of PL intensity for every sample in the 3.3-nm NC set was measured as a function of pH (Fig. 6). In our case, increasing the pH of the sample directly affects the ionic strength of the solution. For a pure NC solution, this results

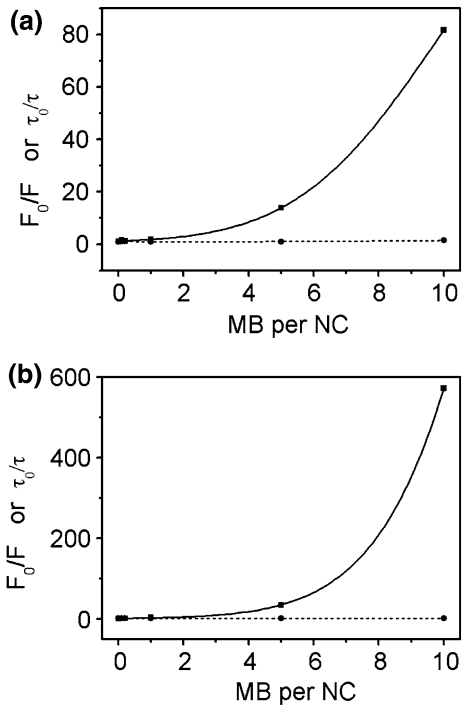

Fig. 5 Stern–Volmer data for NC–MB mixtures. Panels **a** and **b** show intensity (*closed square*, *solid line*) and lifetime (*closed circle*, *dashed line*) Stern–Volmer plots for 2.8-nm and 3.3-nm NC series, respectively. The lifetime SV data is much smaller than the corresponding intensity SV data for both NCs samples, suggesting that static quenching dominates in this system

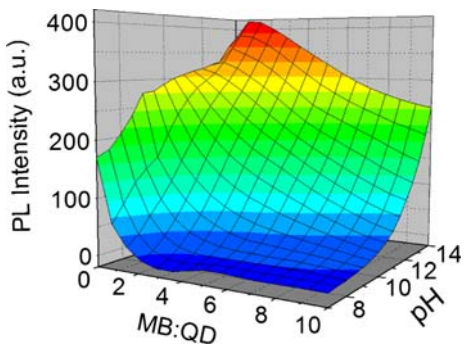

Fig. 6 pH dependence of PL intensity for 3.3-nm NC set. The PL intensity of NCs increases at higher pHs due to better chemical stability. In the presence of MB, complete quenching is not observed for higher pHs even for 10 MB:QD molar ratio because the electrostatic interactions between NCs and MB are altered by high ionic strength

in a better solubility and stability of nanocrystals up to pH of about 11. Consequentially, the PL intensity of CdTe NCs increases. This effect was also seen once MB dye was introduced. However, complete quenching was not achieved for pH above 11. This may be attributed to a lesser association/attraction between MB and NCs due to the increased ionic strength.

Table 2 FCS and zeta measurements results for 2.8-nm nanocrystals' set

Sample name	Diffusion constant ($\mu m^2/s$)	Hydrodynamic size (nm)	Zeta potential (mV)
A	259.6	4.33	−39.1
B	183.3		
C	160.9		
D	158.3		
E	Fluorescence too low: Zeta potential and size measurements were taken instead	4.53	−34.1
F		4.85	−31.3

The diffusion constant was calculated from the FCS curves. It was found to decrease at increasing methylene blue concentrations, which is in accordance with dye molecules adsorbing onto NCs (NCs become heavier). For low fluorescing samples E and F, an increase in the hydrodynamic size of nanocrystals and a decrease in the amplitude of the zeta potential were observed. These results are also in agreement with the adsorption of positively charged methylene blue molecules onto negatively charged nanocrystals' surface

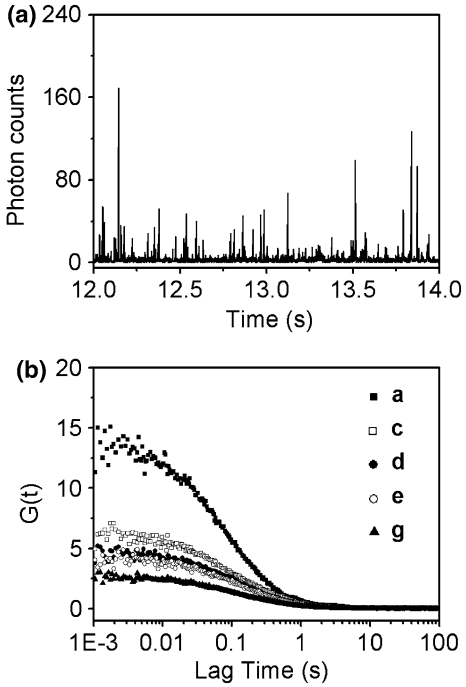

Fig. 7 Fluorescence correlation spectroscopy measurements. Panel **a**. A representative TTTR trace for 3.3-nm NCs. The spikes correspond to NCs emitting photons while they are diffusing through the excitation volume. This data was used to calculate the cross-correlation curves. Panel **b**. Cross-correlation curves for 3.3-nm NC set show a decreasing trend in data. The diffusion constants given in Table 2 were calculated from fits to this data

A more direct confirmation for the adsorption was obtained from NC hydrodynamic size measurements and FCS data. The diffusion constant of nanocrystals, as calculated from the FCS curves (Fig. 7), was found to decrease as a function of increasing MB concentration (Table 2). This corresponds to nanocrystals becoming heavier upon adsorption of MB molecules onto their surface. For samples "e" and "f", the fluorescence levels were too low for the accurate determination of diffusion constant from FCS curves. Therefore, zeta potential and size measurements were taken instead. These showed an increase in the size and a decrease in the amplitude of the surface charge of the nanocrystals (Table 2). Again, this supports the adsorption of positively charged methylene blue molecules onto negatively charged nanocrystals' surface.

Direct Spectroscopic Observation of O_2 [1] by NIR PL

Both energy and charge transfer suggest the increased excitation of MB at wavelengths where the NCs absorb. In terms of the reactive species produced, we expect charge transfer to result in the production of charged molecules and/or radicals. On the other hand, FRET is likely to increase the yield of singlet-MB to triplet-MB transition and thus may increase the efficiency of singlet oxygen production by MB. Both singlet oxygen and oxygen radicals have been linked to cell death [18], which suggests that by adding NCs to the MB solution, the cell kill efficiency of MB can be increased. We have attempted to detect the increase in O_2 [1] production by NIR PL measurements. Only the 3.3-nm NC set was used in these measurements since no FRET was observed for 2.8-nm NC set. The top panel of Fig. 8 shows the NIR PL spectra of samples "f" and "g" of the 3.3-nm NC series at 640-nm excitation. The differential PL signal[1] of these samples (Fig. 8, bottom panel) showed a slight increase in singlet oxygen peak at 1,268 nm upon the addition of a small amount of 3.3-nm NCs to methylene blue solution, confirming our expectations.

HepG2 and HeLa Cell Growth

The final set of experiments was designed to investigate the effect of adding the NC-MB solution on the growth of cancerous cell lines. The first experiments were performed on HepG2 cells. However, very large variations in the number of cells remaining alive after 24-h incubation were observed from well to well, which made it impossible to make any conclusions in regard to cell kill efficiency of our hybrid system. The cause of these variations was the fact the HepG2 cells have a tendency to grow in clusters.

[1] Before the subtraction of "f" and "g" PL spectra, both were corrected for the contribution from the tail of NCs' emission, which had a Gaussian profile in the spectral region in question.

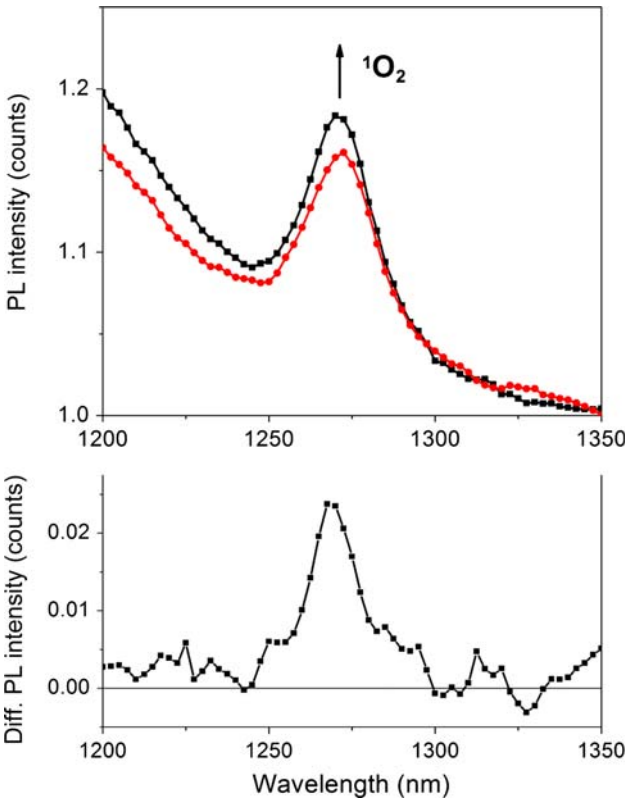

Fig. 8 Direct spectroscopic observation of single oxygen. *Top panel*. NIR photoluminescence spectra shows the evolution of the singlet oxygen peak (1,268 nm) upon the addition of a small amount of 3.3-nm NCs (-■-, sample "3.3 f") to a dilute MB solution (-●-, sample "3.3 g"), as indicated by an arrow. *Bottom panel*: The differential PL signal of the spectra shown in panel **a**. The peak singlet oxygen peak is clearly distinguishable above the noise

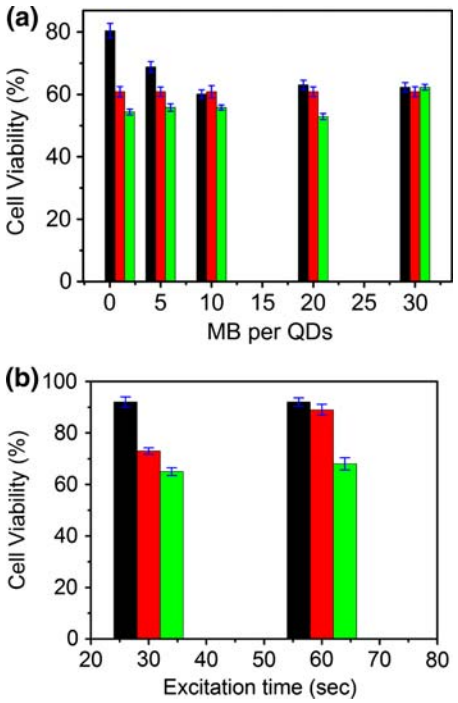

Fig. 9 Cell viability studies involving the incubation of cells in MB–NC-containing mixtures after excitation with UV light. Panels **a** and **b** show the effect of increasing MB:NC ratio (a) and the effect of the time of excitation with UV light (b) on the growth of HeLa cancerous cells (*green bars*). The MB only (*black bars*) and QD only (*red bars*) controls are also shown. All data was normalized to the no NC or MB control sample. The error bars are shown in blue and represent the standard deviation in cell viability within 8 repeat samples. Higher QD:MB molar ratios and longer UV excitations gave best results over the control experiments in terms of the efficiency of MB acting as a photosensitizer

Consequently, the MB and QD solutions, as well as the dye reagent used for cell counting, did not have equal access to all cells. In contrast, HeLa cells preferentially grow in monolayers. This resulted in much smaller variations in counts for any one sample, which allowed us to examine the growth of these cells after being treated by MB and/or NC solutions under UV excitation. Interestingly, for short excitation times ($\sim$30 s) and large MB concentrations (high MB:QD ratio), the presence of NCs seemed to have no effect on cell growth (Fig. 9a). On the other hand, the addition of a small amount of NCs to dilute MB solution leads to a small increase in cell kill efficiency, which was found to be dependent on the excitation time (Fig. 9b).

Conclusions

In solution, methylene blue adsorbs onto the nanocrystal surface with partial dimerization. The dye quenches the NC luminescence primarily via charge transfer, but Förster resonance energy transfer also occurs if there is sufficient overlap between NC emission and MB absorption bands. Both energy and charge transfer imply increased excitation of dye molecules, which suggests that the efficiency of MB to produce reactive oxygen species is also increased. Near-infra red photoluminescence measurements confirmed the increase in the production of singlet oxygen by MB in D_2O, while cell growth studies demonstrated an increase in cell kill efficiency for MB–NC mixtures. These results hint toward the possibility of improving the efficiency of any general photosensitizer utilizing semiconductor nanocrystals.

Acknowledgments This project was partly funded by the Embark Postgraduate Research Scholarship Scheme of the Irish Research Council for Science, Engineering and Technology (IRCSET). Dr. Yuri Gun'ko and Dr. Nikolai Gaponik are acknowledged for their academic assistance.

Open Access This article is distributed under the terms of the Creative Commons Attribution Noncommercial License which permits any noncommercial use, distribution, and reproduction in any medium, provided the original author(s) and source are credited.

References

1. L. Pecci, G. Montefoschi, A. Antonucci, M. Costa, D. Cavallini, Biochem. Biophys. Res. Commun. **301**, 411 (2003)
2. J.P. Tardivo, A.D. Giglio, C.S. de Oliveira, D.S. Gabrielli, H.C. Junqueira, D.B. Tada, D. Severino, R.F. de Turchiello, M.S. Baptista, Photodiagnosis Photodyn. Ther. **2**, 175 (2005)
3. D. Severino, H.C. Junqueira, M. Gugliotti, D.S. Gabrielli, M.S. Baptista, Photochem. Photobiol. **77**, 459 (2003)
4. S.K. Lee, A. Mills, J. Fluorescence **13**, 375 (2003)
5. K. Eichkorn, R. Ahlrichs, Chem. Phys. Lett. **288**, 235 (1998)
6. D.V. Talapin, A.L. Rogach, I. Mekis, S. Haubold, A. Kornowski, M. Haase, H. Weller, Colloids Surf. A **202**, 145 (2002)
7. Y. Li, A. Rizzo, R. Cingolani, G. Gigli, Microchim. Acta. **159**, 207 (2007)
8. A.L. Rogach, *Semiconductor Nanocrystal Quantum Dots Synthesis, Assembly, Spectroscopy and Applications* (Springer, Wien, New York, 2008)
9. S.J. Byrne, S.A. Corr, T.Y. Rakovich, Y.K. Gun'ko, Y.P. Rakovich, J.F. Donegan, S. Mitchell, Y. Volkov, J. Mater. Chem. **16**, 2896 (2006)
10. A.L. Rogach, T. Franzl, T.A. Klar, J. Feldmann, N. Gaponik, V. Lesnyak, A. Shavel, A. Eychmüller, Y.P. Rakovich, J.F. Donegan, J. Phys. Chem. C **111**, 14628 (2007)
11. A. Shavel, N. Gaponik, A. Eychmüller, J. Phys. Chem. B **110**, 19280 (2006)
12. W.W. Yu, L. Qu, W. Guo, X. Peng, Chem. Mater. **15**, 2854 (2003)
13. E. Alphandéry, L.M. Walsh, Y. Rakovich, A.L. Bradley, J.F. Donegan, N. Gaponik, Chem. Phys. Lett. **388**, 100 (2004)
14. A.R. Clapp, I.L. Medintz, H. Mattoussi, Chem. Phys. Chem. **7**, 47 (2006)
15. D. Ramadurai, D. Geerpuram, D. Alexson, M. Dutta, N.A. Kotov, Z. Tang, M.A. Stroscio, Superlat. Microstr. **40**, 38 (2006)
16. M.V. Artemyev, A.I. Bibik, L.I. Gurinovich, S.V. Gaponenko, H. Jaschinski, U. Woggon, Phys. Stat. Sol. B **224**, 393 (2001)
17. P.W. Cyr, M. Tzolov, M.A. Hines, I. Manners, E.H. Sargent, G.D. Scholes, J. Mater. Chem. **13**, 2213 (2003)
18. A. Valencia, J. Morán, Free Radic. Biol. Med. **36**, 1112 (2004)